Research Article

UNIVERSIDAD DE SANTIAGO DE CHILE

Synthesis, structural characterization and antibacterial activity of diorganotin N-(salicylidene)tyrosinates

Laijin Tian*, Lexing Chen, Liping Wang

Key Laboratory of Natural Products and Pharmaceutical Intermediates, Qufu Normal University, Qufu 273165, China. * Corresponding author, e-mail: laijintian@163.com

Received: November 08, 2019; accepted: December 16, 2019

Abstract: Three diorganotin N-(salicylidene)tyrosinates, R_2Sn[2-O-3-X-5-YC_6H_2CH=NCH($CH_2C_6H_4$OH-4)COO] (R, X, Y = Et, H, H (1); *n*-Bu, H, Br (2); *n*-Bu, Br, Br (**3**)), have been synthesized by the one-pot reaction of diorganotin oxide, (*L*)-tyrosine and salicylaldehyde, and characterized by elemental analysis, IR, NMR, and X-ray single crystal diffraction. X-Ray analyses of **1-3** show that the tin atoms of the complexes exhibit distorted trigonal-bipyramidal geometries. The intermolecular O-H···O hydrogen bonds connect the molecules into one-dimensional supramolecular chain or a $R_2^2(20)$ macrocyclic dimer. Bioassay results show that 1-3 have good in vitro antibacterial activity against *Escherichia coli*.

Supporting information: X-Ray (Cif file, Checkcif)

Keywords: *organotin, tyrosine, crystal structure, antibacterial activity.*

1. INTRODUCTION

Schiff bases are easily prepared from condensation reaction of active carbonyl compounds with primary amines. Variation of both the starting aldehyde and the primary amine provides a synthetic strategy that readily allows for fine-tuning of the physicochemical properties of the Schiff base ligand and hence the corresponding metal complexes [1]. The Schiff base derived from α-amino acid and salicylaldehyde displays excellent complexation ability and different mode of coordination to metal ions [2,3]. In recent years, the research about new organotin complexes has been received considerable attention due to their structural diversity and biological properties [4-6]. Some organotin complexes of the Schiff base derived from salicylaldehyde and α-amino acid displayed the monomeric, dimeric, trimeric and polymeric structures and significant cytotoxic activity against some cancer cells [7-13]. The Schiff base derived from salicylaldehyde and *L*-tyrosine, *N*-(salicylidene)tyrosine, is a multidentate ligand with two hydroxyls, one imine, and one carboxyl group. The synthesis, structure and properties of the organotin complexes based on this ligand need to be further studied and expanded although several of its diorganotin complexes have been reported [8,12,13]. For this purpose, we synthesized three diorganotin *N*-(salicylidene)tyrosinates by the one-pot three-component reaction, R_2Sn[2-O-3-X-5-YC_6H_2CH=NCH(-$CH_2C_6H_4$OH-4)COO] (R, X, Y = Et, H, H (**1**); *n*-Bu, H, Br (**2**); *n*-Bu, Br, Br (**3**)), and determined their crystal structures and antibacterial activity against *Escherichia coli* (Scheme 1).

2. EXPERIMENTAL

2.1 Materials and physical measurements

The chemicals were of reagent grade and were used without further purification. Carbon, hydrogen and nitrogen analyses were obtained using a Perkin Elmer 2400 Series II elemental analyzer. The melting points were measured on a WRS-1A digital melting point apparatus. IR spectra were recorded on a Nicolet 470 FT-IR spectrophotometer using KBr discs in the range 4000-400 cm-1. ^{1}H and ^{13}C NMR spectral data were collected using a Bruker Avance III HD 500 MHz NMR spectrometer with $CDCl_3$ or DMSO-d^6 as solvent and TMS as internal standard.

2.2 Synthesis of the complexes

L-tyrosine (0.362 g, 2 mmol), diorganotin oxide (2 mmol) (for Et_2SnO 0.386 g, for *n*-Bu_2SnO 0.498 g), and salicylaldehyde (0.244 g, 2 mmol) [or 5-bromosalicyaldehyde (0.402 g, 2 mmol) or 3,5-dibromosalicyaldehyde (0.560 g, 2 mmol)] were mixed in 70 mL of anhydrous methanol-chloroform (1:1, V/V). The reac-

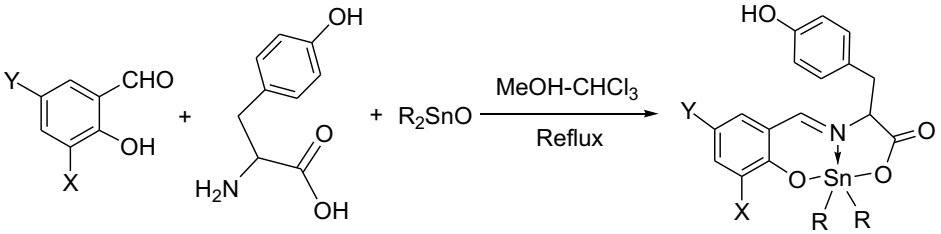

R, X, Y = Et, H, H (**1**), *n*-Bu, H, Br (**2**); *n*-Bu, Br, Br (**3**)

Scheme 1. Synthesis of the complexes.

tion mixtures were refluxed under electromagnetic stirring for 8 h. The yellow solution obtained was cooled and filtered, and the solvent was removed under reduced pressure using a rotary evaporator. The resulting yellow solid was recrystallized from methanol.

$Et_2Sn[2\text{-}OC_6H_4CH{=}NCH(CH_2C_6H_4OH\text{-}4)COO]$ (**1**):

Yield 0.80 g (87%), m.p. 222˚C (literature value [13] 225˚C). ^{1}H NMR (DMSO-d_6) δ: 0.98 (t, J = 8.0 Hz, $J(^{119}Sn\text{-}^1H)$ = 128 Hz, 3H, CH_3), 1.00-1.19 (m, 7H, $2SnCH_2{+}CH_3$), 2.97 (dd, J = 7.0, 14.0 Hz, 1H, ArCHH), 3.24 (dd, J = 4.5, 14.0 Hz, 1H, ArCHH), 4.30 (dd, J = 4.5, 7.5 Hz, 1H, N-CH), 6.63 (d, J = 8.5 Hz, 2H, H-3 of C_6H_4OH), 6.65-6.68 (m, 2H, H-5 and H-6 of C_6H_4), 7.11 (dd, J = 2.0, 8.0 Hz, 1H, H-3 of C_6H_4), 6.89 (d, J = 8.5 Hz, 2H, H-2 of C_6H_4OH), 7.40 (ddd, J = 2.0, 7.5, 8.5 Hz, 1H, H-4 of C_6H_4), 8.19 (s, $J(^{119}Sn\text{-}1H)$ = 42 Hz, 1H, CH=N), 9.28 (s, 1H, OH) ppm.

$n\text{-}Bu_2Sn[5\text{-}Br\text{-}2\text{-}OC_6H_3CH{=}NCH(CH_2C_6H_4OH\text{-}4)COO]$(**2**):

Yield 1.07 g (90%), m.p. 195˚C ((literature value [13] 193˚C). ^{1}H NMR (DMSO-d_6) δ: 0.74 (t, J = 7.5 Hz, 3H, CH_3), 0.83 (t, J = 7.5 Hz, 3H, CH_3), 0.87-0.93 (m, 2H, CH_2), 1.15-1.25(m, 6H, $3CH_2$), 1.32-1.38 (m, 4H, $2CH_2$), 3.07 (dd, J = 5.5, 14.0 Hz, 1H, ArCHH), 3.20 (dd, J = 5.0, 14.0 Hz, ^{1}H, ArCHH), 4.32 (dd, J = 5.0, 5.5 Hz, ^{1}H, N-CH), 6.62 (d, J = 9.0 Hz, ^{1}H, H-3 of C_6H_3Br), 6.63 (d, J = 8.5 Hz, 2H, H-3 of C_6H_4OH), 6.84 (d, J = 8.5 Hz, 2H, H-2 of C_6H_4OH), 7.43 (d, J = 2.5 Hz, 1H, H-6 of C_6H_3Br), 7.48 (dd, J = 2.5, 9.0 Hz, 1H, H-4 of C_6H_3Br), 8.40 (s, $J(^{119}Sn\text{-}1H)$ = 45 Hz, 1H, CH=N), 9.28 (s, 1H, OH) ppm.

$n\text{-}Bu_2Sn[3,5\text{-}Br\text{-}2\text{-}OC_6H_2CH{=}NCH(CH_2C_6H_4OH\text{-}4)COO]$ (**3**):

Yield 1.25 g (93%), m.p. 187˚C. Anal. calcd for $C_{24}H_{29}Br_2NO_4Sn$: C 42.77, H 4.34, N 2.08; found C 42.79, H 4.24, N 2.09%. IR (KBr): 3387 [ν(OH)], 1649 [ν(COO)as], 1617 [ν(C=N)], 1491, 1383 [(COO)s], 1367, 1219, 1132, 1025 cm^{-1}. ^{1}H NMR ($CDCl_3$) δ: 0.85 (t, J = 7.5 Hz, 3H, CH_3), 0.98 (t, J = 7.5 Hz, 3H, CH_3), 1.25-1.77 (m, 12 H, $2SnCH_2CH_2CH_2$), 2.99 (dd, J = 9.0, 14.0 Hz, 1H, ArCHH), 3.46 (dd, J = 3.5, 14.0 Hz, 1H, ArCHH), 4.18 (dd, J = 3.5, 9.0 Hz, 1H, N-CH), 6.15 (s, br., OH), 6.81 (d, J = 8.0 Hz, 2H, H-3 of C_6H_4OH), 6.96 (d, J = 8.0 Hz, 2H, H-2 of C_6H_4OH), 6.98 (d, J = 2.5 Hz, 1H, H-4 of $C_6H_2Br_2$), 7.49 (s, $J(^{119}Sn\text{-}H)$ = 44 Hz, 1H, CH=N), 7.83 (d, J = 2.5 Hz, 1H, H-6 of $C_6H_2Br_2$) ppm. ^{13}C NMR ($CDCl_3$) d: 173.19 (COO), 170.91 (C=N), 163.61 (C-2 of $C_6H_2Br_2$), 155.80 (C-4 of C_6H_4OH), 141.96 (C-4 of $C_6H_2Br_2$), 135.93 (C-6 of $C_6H_2Br_2$), 131.35 (C-2 of C_6H_4OH), 126.20 (C-1 of C_6H_4OH), 118.24 (C-1 of $C_6H_2Br_2$), 118.03 (C-3 of $C_6H_2Br_2$), 116.21 (C-3 of C_6H_4OH), 107.45 (C-5 of $C_6H_2Br_2$), 70.60 (N-C), 41.19 ($ArCH_2$), 26.92 (C-β), 26.67 (C-β´), 26.66 (C-γ), 26.57 (C-γ´), 22.52 (C-α), 22.19 (C-α´), 13.65 (C-δ), 13.48 (C-δ´) ppm.

2.3 X-ray crystallography

The yellow single crystals of **1-3** was obtained from dichloromethane-methanol (1:1, V/V) by slow evaporation at room temperature. Diffractions measurements were performed on a Bruker Smart Apex imaging-plate area detector fitted with graphite monochromatized Mo-Kα radiation (0.71073 Å) using the φ and ω

Table 1. Crystallographic and refinement data of complexes

Compound	**1**	**2**×CH_2Cl_2	**3**
Empirical formula	$C_{20}H_{23}NO_4Sn$	$C_{25}H_{32}BrCl_2NO_4Sn$	$C_{24}H_{29}Br_2NO_4Sn$
Formula weight	460.08	680.02	673.99
Crystal system	Orthorhombic	Triclinic	Monoclinic
Space group	*P*bca	*P*-1	$P2_1/n$
a /Å	14.715(4)	10.851(7)	8.704(2)
b /Å	7.692(2)	11.141(7)	30.117(7)
c /Å	34.902(10)	13.887(9)	10.344(2)
α /(°)	90	70.558(13)	90
b /(°)	90	72.038(12)	102.223(6)
g /(°)	90	68.777(13)	90
Volume /Å^3	3950.5(19)	1441.6(16)	2650.0(10)
Z	8	2	4
D_c / (g×cm^{-3})	1.547	1.567	1.689
m / mm^{-1}	1.317	2.487	4.008
F(000)	1856	680	1328
q range /(°)	1.2 to 25.0	2.0 to 25.2	2.1 to 26.0
Crystal size / mm	0.16x0.14x0.01	0.50x0.40x0.30	0.42x0.10x0.08
Tot. reflections	25549	8019	16909
Uniq. Reflections, R_{int}	3470, 0.109	5066, 0.071	5208, 0.049
R_1 indices [I>2σ(I)]	0.143	0.080	0.048
wR_2 indices (all data)	0.307	0.206	0.118
$\Delta\rho_{min}$, $\Delta\rho_{max}$/(e·Å^{-3})	-0.910, 0.999	-1.734, 1.388	-0.629, 0.770

scan technique. The structures were solved by direct-methods and refined by a full-matrix least squares procedure based on F^2 using SHELXL-97 [14]. The non-hydrogen atoms were refined anisotropically and hydrogen atoms were placed at calculated positions in the riding model approximation. In 1, a ethyl

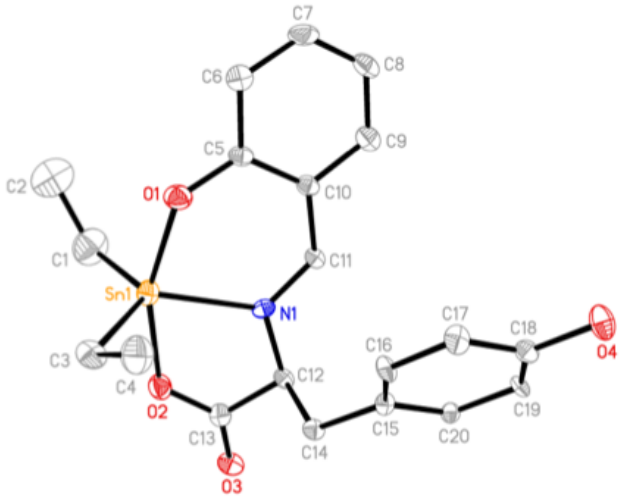

Figure 1. The molecular structure of 1. Hydrogen atoms are omitted for clarity.

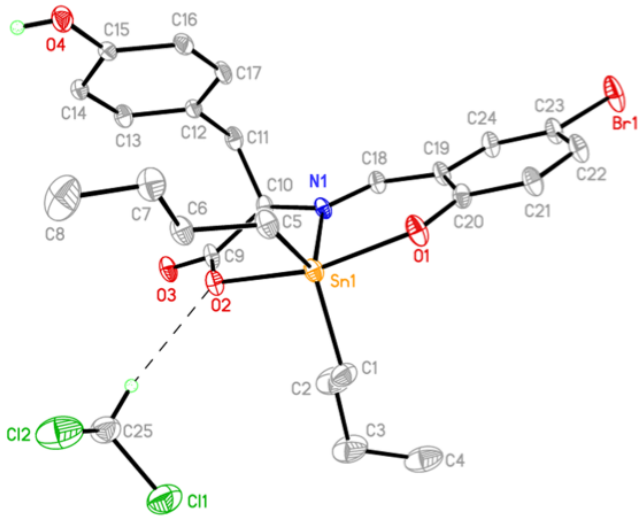

Figure 2. The molecular structure of 2. Only H(4) and H(25A) are given for clarity.

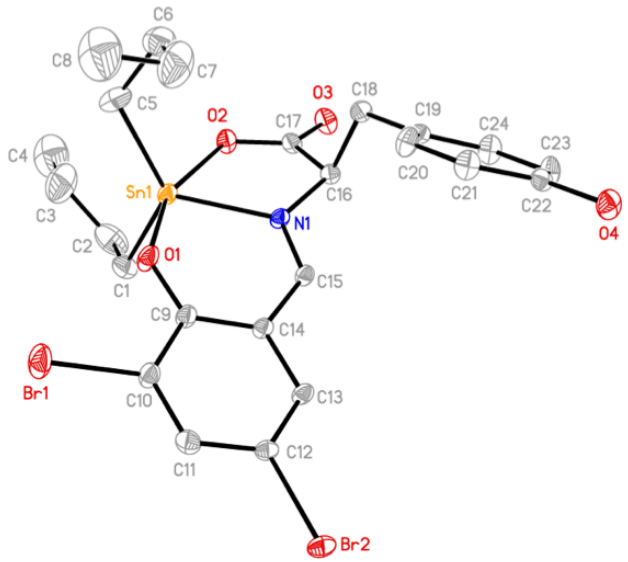

Figure 3. The molecular structure of 3. Hydrogen atoms are omitted for clarity.

(C(3)-C(4)) was disordered over two conformations, the site occupancies were refined to 0.55(2):0.45(2). In **2** and **3**, the site occupancies were refined to 0.67(3):0.33(3), 0.60(2):0.40(2), and 0.82(2):0.18(2), respectively, for the disorderly butyls. In refinements, the C-C bonds and 1,3-distances of the disorderly butyl groups were restrained to 1.52(1) and 2.52(2) Å, respectively. The Crystal data, collection procedures and refinement results are shown in Table 1. The crystallographic data of 1-3 have been deposited with the Cambridge Crystallographic Data Centre as supplementary publication number CCDC 1588973, 1964182, and 1964183.

2.4 Antibacterial activity

The antibacterial activity of the complexes against *Escherichia coli* was determined by microcalorimetric method according to the literature [15]. A 2277 Thermal Activity Monitor (Thermometric AB, Sweden) was used to determine the power-time curves of bacterial growth at 310*K*. The growth rate constants (μ) at different concentrations (C) of organotin drugs **1-3** are listed in Table 2. The relationship between the growth rate constants (μ) and concentration (C) of organotin drug was fitted by using computer, and the linear regression equations for **1-3** are as follows: $\mu = -0.00400C+0.06959$ ($R = 0.98$), $\mu = -0.00616C+0.07197$ ($R = 0.99$), and $\mu = -0.00546C+0.06708$ ($R = 0.96$). When the growth rate constant is 0, the minimum inhibitory concentration (MIC) was confirmed.

3. RESULTS AND DISCUSSION

Complexes **1-3** were prepared from the one-pot reaction of diorganotin oxide, (*L*)-tyrosine and salicylaldehyde in a 1:1:1 molar ratio in methanol-chloroform (1:1, v/v) mixed solvent with yields of 87-93% (Scheme 1). Compared with the two-step method [7-9] in which the Schiff base carboxylic acid ligand needs to be first prepared, this preparation process is simpler and highly efficient.

The IR of **3** showed a strong broad band at 3387 cm^{-1} assigned to phenolic ν(OH) of tyrosyl residue. The difference between ν_{as}(COO) and ν_s(COO) bands, Δν(COO), is 266 cm^{-1}, suggesting that the carboxylate is coordinated to tin in a monodentate mode [16]. This monodentate coordination mode is further confirmed by the shown below X-ray structures. In ^{1}H NMR spectra of the complexes, the signal assigned to azomethine proton CH=N appear at ~8.3 ppm in DMSO-d_6 (**1** and **2**) and 7.49 ppm in $CDCl_3$ (**3**). The spin-spin coupling between the azomethine proton and the tin nucleus, $^3J(^{119}Sn\text{-}^1H)$, is in the range of 42-45 Hz, confirming that there exist the C=N®Sn coordination in the solution in **1-3**. The complexes display two sets of ^{1}H and ^{13}C NMR signals from the R_2Sn (R = Et, Bu) moieties indicating that the two R groups experience different environments on the NMR time scale due to the presence of the rigid chelate ring around tin and a stereogenic carbon in the ligand [9,17]. The molecular structure of **1-3** is shown in Figures 1-3, and selected geometric parameters are given in Table 3. In **1-3**, the coordination geometry of the tin atom is a distorted trigonal

Table 2. Growth rate constants (μ) at different concentrations (C) of **1-3.**

1						
C (μg/ml)	0	1.25	2.50	3.75	5.00	6.25
μ (min^{-1})	0.07053	0.06352	0.05833	0.05566	0.05076	0.04372
2						
C (μg/ml)	0	1.25	2.50	3.75	5.00	6.25
μ (min^{-1})	0.07053	0.06621	0.05536	0.05004	0.04192	0.03230
3						
C (μg/ml)	0	1.25	2.50	3.75	5.00	6.25
μ (min^{-1})	0.07053	0.05736	0.05116	0.04695	0.04022	0.03386

bipyramid with two carbons of alkyl groups and a N(1) atom from the ligand defining the trigonal plane and a phenolic O(1) and a monodentate carboxylate O(2) atom occupying the axial positions. The Sn(1)-O(1) distances (2.067(13)-2.100(6) Å) is shorter than Sn(1)-O(2) distances (2.153(14)-2.210(6) Å), and the bond angles of the axial positions, O(1)-Sn(1)-O(2), are in the range of 157.15(15)°-159.4(5)°. The tin atom forms a five- and a six-membered chelate rings with the ONO tridentate ligand, and the O(1)-Sn(1)-N(1) (82.47(14)-84.9(5)°) and O(2)--Sn(1)-N(1) (74.6(5)-74.8(2)°) angles have a serious deviation from the ideal angle of 90°. The monodentate mode of coordination of carboxylate is also reflected in two disparate C-O bond lengths of the carboxylate. For example, in **3**, the distances of C(17)-O(2) and C(17)-O(3) bonds are 1.287(6) and 1.221(6) Å, respectivly. These structural features are comparable with those observed in [3-CH_3O-2-OC_6H_3CH=NCH(CH_2Ph)COO]$SnEt_2$ [18], [2-O-5-BrC_6H_3CH=NCH($CH_2C_6H_4OH$-4)COO]$SnEt_2$ [13], [3,5-Br_2-2-OC_6H_2-CH=NCH(CH_2Ind)COO]$SnBu_2$ [10], and [2-OC_6H_4CH=NCH($CH(CH_3)_2$)COO]$SnCy_2$ [19].

In the complexes, there exist the intermolecular O-H···O hydrogen bonds between the phenolic hydroxyl O-H of tyrosyl residue and uncoordinated carbonyl O(3) atom from the adjacent ligand (Table 4). In **1** and **3**, the hydrogen bonds connect the molecules into one-dimensional supramolecular chain with Sn×××Sn distances of 14.292(2) (**1**) and 10.344(2) Å (**3**), respectively (Figure 4). In **2**, there is a centrosymmetric $R_2^2(20)$ macrocycle with Sn···Sn distances of 10.607(2), and the macrocycles are further linked by a pair of C(10)-H(10)···O(3) hydrogen bonds to form a one-dimensional supramolecular chain (Table 4, Figure 5).

The antibacterial activity of the complexes and the reference drug (penicillin sodium and cefazolin sodium) was listed in Table 5. The results showed that the complexes against *Escherichia coli* are active and more active than the reported dibutyltin *N*-(salicylidene)tyrosinate (MIC 20.34 μg·mL^{-1}) [13], dicyclohexyltin *N*-(salicylidene)valinate (MIC 23.11 μg·mL^{-1}) [19], and dibutyltin *N*-(2-hydroxyl-1-naphthmethylene)glycinate (MIC 25 μg·mL^{-1}) [20]. They can be considered as anti-bacterial compounds to further study and modified although the activity of the complexes is lower than that of the reference drugs.

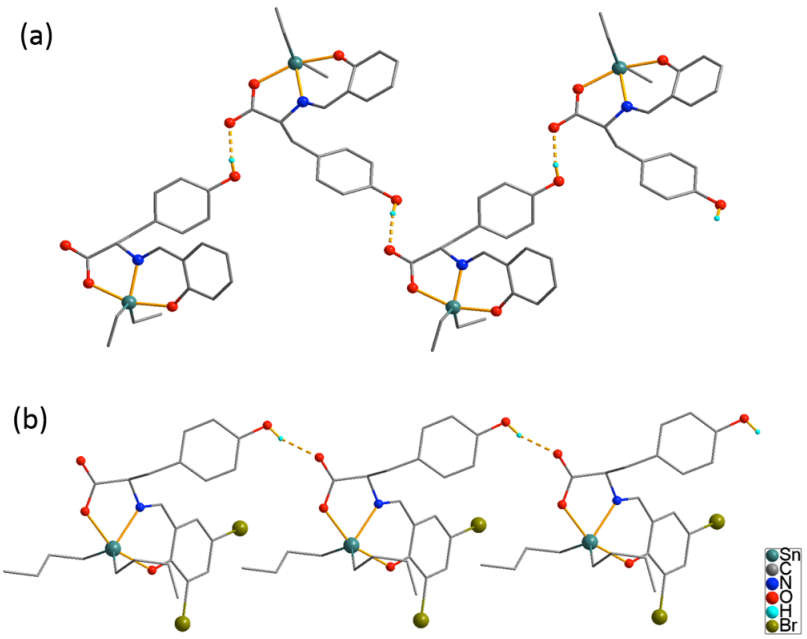

Figure 4. The 1D supramolecular chain in 1 (a) and 3 (b) formed by the O-H···O hydrogen bonds. Only hydrogen atoms of hydroxyls are given for clarity.

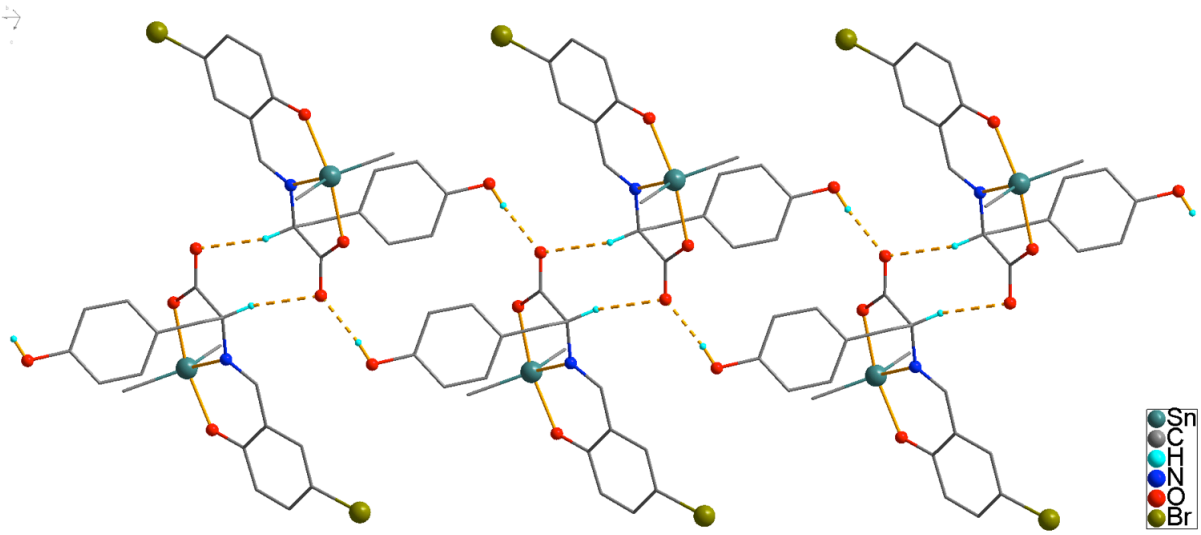

Figure 5. The $R_2^2(20)$ macrocycle dimer and supramolecular chain in 2 formed by the O-H···O and C-H···O hydrogen bonds. Only one carbon atom of butyl and hydrogen atoms involving hydrogen bonds are given for clarity.

Table 3. Selected bond lengths (Å) and angles (°) for the complexes.

	1	**2**×CH_2Cl_2	**3**
Sn(1)-C(1)	2. 131(19)	2.125(10)	2.117(6)
Sn(1)-C(n)	2.15(2)	2.119(9)	2.107(7)
Sn(1)-N(1)	2.157(12)	2.174(6)	2.175(4)
Sn(1)-O(1)	2.067(13)	2.100(6)	2. 098(4)
Sn(1)-O(2)	2.153(14)	2.210(6)	2.161(4)
O(1)-Sn(1)-C(1)	97.8(6)	97.6(4)	95.4(2)
O(1)-Sn(1)-O(2)	159.4(5)	158.7(2)	157.15(15)
C(1)-Sn(1)-O(2)	92.5(6)	91.4(4)	95.2(2)
O(1)-Sn(1)-C(n)	86.7(10)	92.4(3)	93.7(2)
C(1)-Sn(1)-C(n)	135.4(12)	130.8(4)	127.0(3)
O(2)-Sn(1)-C(n)	98.1(15)	96.3(3)	96.0(3)
O(1)-Sn(1)-N(1)	84.9(5)	83.9(2)	82.47(14)
C(1)-Sn(1)-N(1)	115.6(7)	109.2(3)	112.1(2)
O(2)-Sn(1)-N(1)	74.6(5)	74.8(2)	74.80(14)
C(n)-Sn(1)-N(1)	109.0(11)	119.7(3)	120.9(3)

n = 3 for **1**, 5 for **2** and **3**

Table 4. H-Bonding geometry parameters (Å, °) for the complexes

Compound	D-H···A	D-H (Å)	H···A (Å)	D···A (Å)	D-H···A (°)	Symmetry codes i
1	O(4)-H(4)···O(3)^i	0.82	1.87	2.649(2)	159	*x*-1/2, *y*, -*z*+1/2
2×CH_2Cl_2	O(4)-H(4)···O(3)^i	0.82	1.93	2.716(2)	160	-*x*+1, -*y*+1, -*z*
	C(10)-H(10)···O(3)^i	0.98	2.40	3.323(2)	157	-*x*+, -*y*+1, -*z*
	C(25)-H(25A)···O(2)	0.97	2.56	3.518(2)	171	
3	O(4)-H(4)···O(3)^i	0.82	1.92	2.701(1)	159	*x*, *y*, *z*+1

Table 5. Antibacterial activity (MIC, μg·mL^{-1}) of the complexes[a]

Complex	**1**	**2**	**3**	Penicillin sodium	cefazolin sodium
Escherichia coli	17.40	11.68	12.28	8.03	2.01

[a] MIC = minimum inhibitory concentration.

Acknowledgments

This work was supported by the Undergraduate Innovation Project of Qufu Normal University (No. 2018A045), and Shandong Provincial Natural Science Foundation, China (No. ZR2013BM007).

REFERENCES

[1] Liu, X.; Manzur, C.; Novoa, N. *Coord. Chem. Rev.* **2018**, 357, 144-172. DOI: 10.1016/j.ccr.2017.11.030.

[2] Muche, S.; Levacheva, L.; Samsonova, O.; Pham, L.; Christou, G.; Bakowsky, U.; Holynska, M. A chiral, low-cytotoxic [Ni_{15}]-wheel complex. *Inorg. Chem.* **2014**, 53, 7642-7649. DOI: 10.1021/ic500957y.

[3] Muche, S.; Harms, K.; Biernasiuk, A.; Malm, A.; Popiolek, L.; Hordyjewska, A.; Olszewska, A.; Holynska, M. *Polyhedron* **2018**, 151, 465-477. DOI: 10.1016/j.poly.2018.05.056.

[4] Davies, A.G.; Gielen, M.; Pannell, K.H.; Tiekink, E.R.T. *Tin Chemistry***:** *Fundamentals, Frontiers, and Applications*. John Wiley& Sons, Chichester, U.K., 2008. DOI: 10.1002/9780470758090.

[5] Baul, T.S.B. *Appl. Organometal. Chem.* **2008**, 22, 195-204. DOI: 10.1002/aoc.1378.

[6] Bantia, C.N.; Hadjikakou, S.K.; Sismanoglu, T.; Hadjiliadis, N. *J. Inorg. Biochem.* **2019**, 194, 114-152. DOI: 10.1016/j.jinorgbio.2019.02.003.

[7] Baul, T.S.B.; Masharing, C.; Ruisi, G.; Jirasko, R.; Holcapek, M.; Vos, D.; Wolstenholme, D.; Linden, A. *J. Organomet. Chem.* **2007**, 692, 4849-4862. DOI: 10.1016/j.jorganchem.2007.06.061.

[8] Baul, T.S.B.; Kehie, P.; Duthie, A.; Hopfl, H. *J. Organomet. Chem.* **2017**, 828, 96-105. DOI: 10.1016/j.jorganchem.2016.11.028.

[9] Baul, T.S.B.; Kehie, P.; Duthie, A.; Guchhait, N.; Raviprakash, N.; Mokhamatam, R. B.; Manna, S. K.; Armata, N.; Scopelliti, M.; Wang, R.; Englert, U. *J. Inorg. Biochem.* **2017**, 168, 76-89. DOI: 10.1016/j.jinorgbio.2016.12.001.

[10] Tian, L.; Liu, X.; Zheng, X.; Sun, Y.; Yan, D.; Tu L. *Appl. Organometal. Chem.* **2011**, 25, 298-304. DOI: 10.1002/aoc.1758.

[11] Tian, L.-J.; Chen, L.-X.; An, W.-G.; Liu, X.-C. *Chinese J. Struc. Chem.* **2019**, 38, 1977-1985. DOI: 10.14102/j.cnki.0254-5861.2011-23788.

[12] Tian, L.; Han, L.; Yao, Y.; Zheng, X.; **Liu, X.**; **Lin**, X. *Appl. Organometal. Chem.* **2018**, *32*, e4475. DOI: 10.1002/aoc.4475.

[13] Lin, Y.; An, W.; Ge, X.; Liu, M.; Wang, Y.; Liu, X.; Tian, L. *J. Coord. Chem.* **2019**, 72, 987-1001. DOI: 10.1080/00958972.2019.1584796.

[14] Sheldrick G.M. A short history of SHELX. *Acta Crystallogr. A,* **2008**, 64, 112-122. DOI: 10.1107/S0108767307043930.

[15] Zhang, H.; Yu, X.; Li, X.; Pan, X. Thermochim. Acta 2004, 416, 71-74. DOI: 10.1016/j.tca.2003.11.033.

[16] Deacon, G. B. and Phillips R. J. *Coord. Chem. Rev.* **1980**, 33, 227-250. DOI: 10.1016/S0010-8545(00)80455-5.

[17] Tian, L.; Yao, Y.; Wang, Y.; Liu, J. *J. Mol. Struct.* **2018**, 1156, 441-449. DOI: 10.1016/j.molstruc.2017.11.132.

[18] Liu, Q.; Zhang, H.; Zheng, X.; Wang, W.; Tian, L. *Appl. Organometal. Chem.* **2016**, 30, 630-637. DOI: 10.1002/aoc.3480.

[19] Shi, X.; Kong, G.; Liu, L.; Gao, H.; Gao, X.; Tian L. *Commun. Inorg. Synth.* **2016**, 4, 12-16. DOI: 10.21060/cis.2016.421

[20] Nath, M.; Yadav, R.; Gielen, M.; Dalil, H.; Vos, D. D.; Eng, G. *Appl. Organometal. Chem.* **1997**, 11, 727-736. DOI: 10.1002/(SICI)1099-0739(199709)11:9<727::AID-AOC-639>3.0.CO;2-X.

Communications in Inorganic Synthesis is sponsored and supported by: Universidad de Santiago de Chile.